SOLUTION MINING RESEARCH INSTITUTE
105 Apple Valley Circle
Clarks Summit, PA 18411, USA

Telephone: +1 570-585-8092
Fax: +1 505-585-8091
www.solutionmining.org

Technical Conference Paper

Creep closure rate of a shallow salt cavern

Pierre Bérest, Jean-François Beraud, Vincent de Greef
LMS, Ecole Polytechnique, Palaiseau

Benoît Brouard, Brouard Consulting, Paris, France

Emmanuel Hertz, Cédric Lheur
CSME, Levallois-Perret, France

SMRI Spring 2011 Technical Conference
18 – 19 April 2011
Galveston, Texas, USA

Solution Mining Research Institute Spring 2011 Technical Conference
Galveston, Texas, USA, 18 – 19 April 2011

CREEP CLOSURE RATE OF A SHALLOW CAVERN

Pierre Bérest, Jean-François Beraud, Vincent de Greef
LMS, Ecole Polytechnique, Palaiseau, France

Benoit Brouard, Brouard Consulting, Paris, France

Emmanuel Hertz, Cédric Lheur
Compagnie des Salins du Midi et des Salines de l'Est, Levallois-Perret, France

Abstract

Cavern creep closure rate was recorded in the SG13-SG14 salt cavern of the Gellenoncourt brine field operated by CSME at Gellenoncourt in Lorraine, France. Cavern compressibility and the evolution of cavern brine temperature first were measured. In this shallow cavern (250-m, or 800-ft, deep), which had been kept idle for 30 years, cavern-brine thermal expansion can be disregarded. To assess cavern closure rate, a 10-month brine-outflow test was performed, followed by a 6-month shut-in test. During the tests, brine outflow or pressure evolution is influenced by atmospheric pressure changes, ground temperature changes and Earth tides. From the average pressure-evolution rate, it can be inferred that the steady-state cavern closure rate is slower than 10^{-5}/yr (0.001%/yr, or 3×10^{-13} /s.)

A part of the material used to write this paper was already included in a paper presented during the Grand Junction SMRI Meeting. The update includes the analyses of atmospheric pressure effects, dynamic oscillations of the brine column, column temperature changes and brine crystallization.

Key words: Cavern abandonment, in situ test, salt creep

Introduction

In the long term, salt behaves as a viscous fluid and caverns gradually shrink. Deep caverns have experienced creep closure rates by several percent per year, as proved by direct measurement of cavern-shape evolution through sonar surveys. Creep rates in shallow caverns are much slower and must be assessed through *shut-in pressure tests*, which consist of closing the cavern and measuring the pressure evolution at the wellhead as a function of time, or through *brine outflow tests*, which consist of opening the cavern and measuring the flow of fluid (brine or hydrocarbon) expelled from the wellhead. For instance, Bérest et al. (2001) measured a cavern-closure rate of $\dot{\varepsilon}_{cr} = \dot{V}/V = -3\times10^{-4}$/yr (or - 0.03%/yr) in a 950-m deep cavern at Etrez, France; Brouard et al. (2004) observed a convergence rate of $\dot{\varepsilon}_{cr} = \dot{V}/V = -10^{-3}$/yr (or - 0.1%/yr) in a 700-m deep cavern at Carresse, France.

In this paper, we describe two such tests (Figures 1 and 2) performed in the 250-m deep SG13-14 cavern of the Gellenoncourt brine-field operated by Compagnie des Salins du Midi et Salines de l'Est (CSME) in Lorraine, France. The objective of these tests was to assess long-term cavern closure rate. Cavern closure rate in such a shallow cavern is exceedingly slow, which raises specific measurement problems.

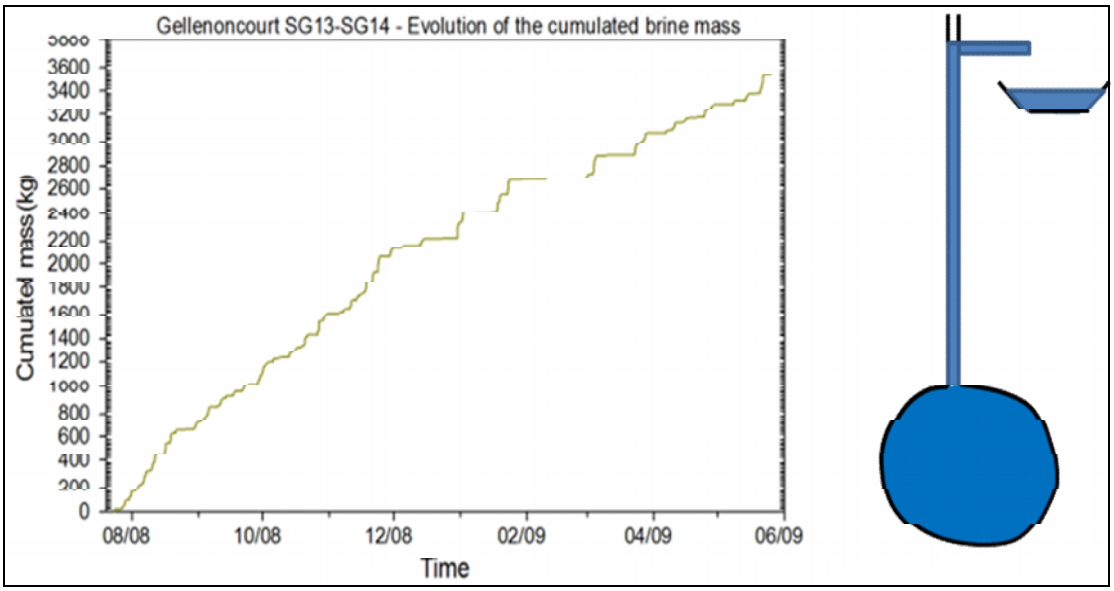

Figure 1 - Brine outflow test (July 23, 2008 to May 25, 2009).

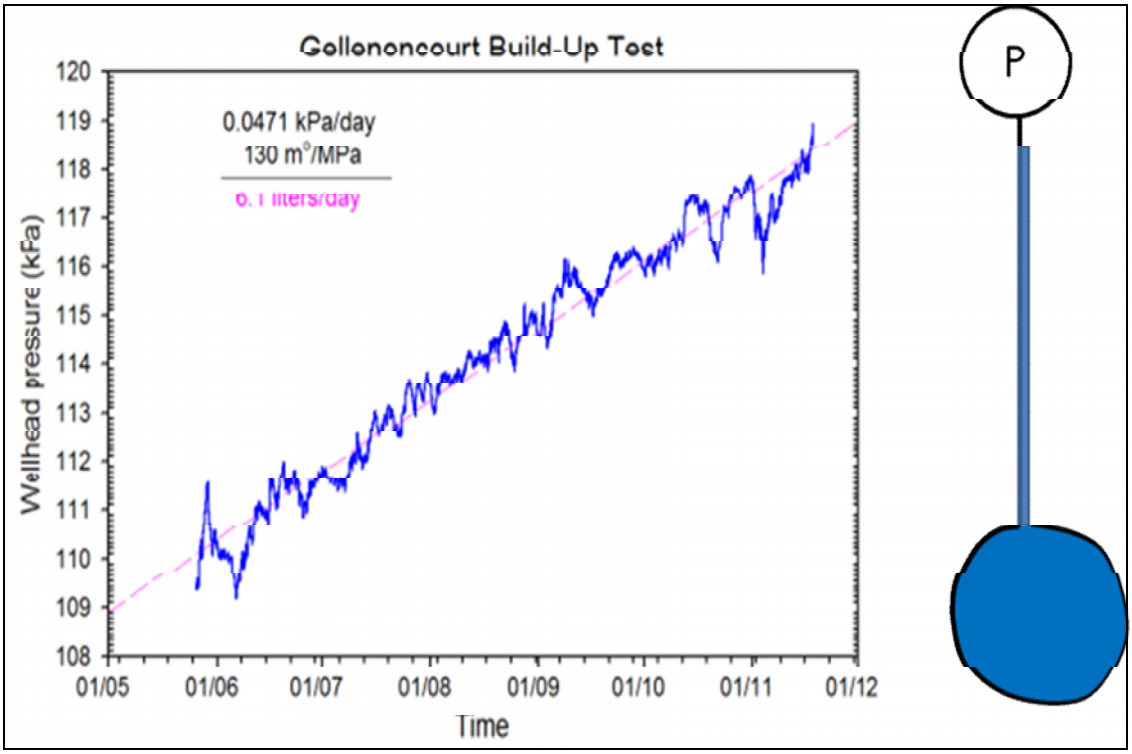

Figure 2 -Shut-in pressure test (May 25, 2009 to November 19, 2009).

2. THE SG13-14 CAVERN

2.1. Cavern volume

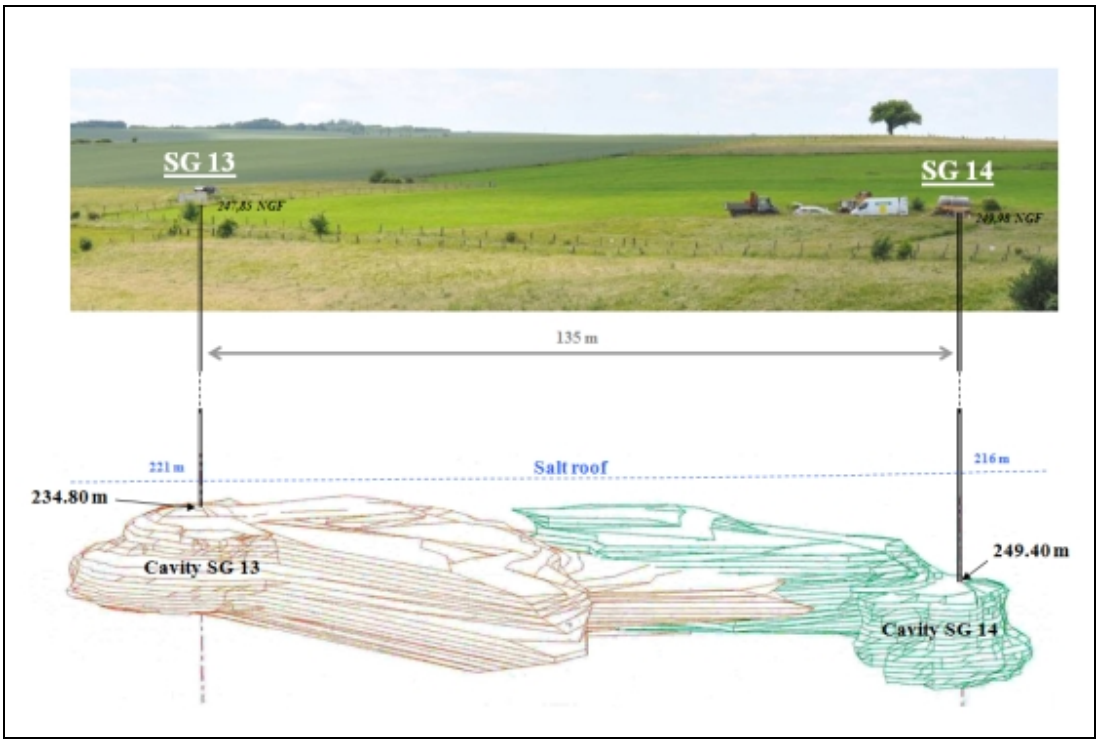

Figure 3 – 3D view of the SG13-SG14 cavern (From November 2000 sonar survey: the cavern is viewed from East to West with a 10° downward dip angle.)

CSME has operated a brine field at Gellenoncourt in Eastern France since the beginning of the 20th Century; this brine field, described in Buffet (1998) is located at the eastern (and shallowest) edge of the Keuper bedded-salt formation of Lorraine-Champagne, in which the salt thickness is 150 m. Five horizontal "salt pencils" have been described by geologists. The salt content of this field is highest in the first (shallowest) and third pencils.

During the first half of the 20th Century, single wells were brined out. After 1965, the hydro-fracturing technique was used. For this brine field, cased and cemented wells are drilled to a depth of 280-300 m — i.e., at the base of the third pencil. The horizontal distance between two neighboring wells typically is 100 to 150 m. Through hydro-fracturing, a link is created between two such caverns at the base of the third pencil. Water then is injected in one well, and brine is withdrawn from the other well. After some time, the injection and withdrawal wells are switched. The caverns grow, and their roofs actually reach the first pencil. Brining stops when the cavern roof is 10 m below the salt roof. This 10-m-thick salt slab is left to protect the overlying strata, which are prone to weathering when in contact with brine.

In 2007, CSME decided to perform tests to gain a better knowledge of cavern long-term mechanical behavior. The SG13-SG14 cavern was selected for performing in-situ tests, as this cavern is representative of the field and had been kept idle for a long period of time. The SG13 and SG14 7''-wells were operated as brine-production caverns from July 1976 to July 1980. After some time, the two caverns coalesced, and, in 1980, SG13-SG14 was composed of two parts connected by a large link, see Figure 3. Cavern volume was measured through sonar surveys; it is V = 240,000 m^3.

2.2. Cavern compressibility

Cavern compressibility is the ratio between the injection (or withdrawal) rate *q* and the cavern pressure change rate $\dot{P}$ during a rapid injection (or withdrawal), or $q = \beta V \dot{P}$. It is proportional to cavern volume, or *V*, and it is related to the elastic (adiabatic) properties of the rock mass and of the fluids contained in the cavern (Bérest et al., 1999). SG13-SG14 compressibility, as measured on July 3, 2008, is $\beta V = 130$ m^3/MPa, from which a $\beta = 5.4\times10^{-4}$/MPa cavern compressibility coefficient can be inferred.

2.3. Cavern temperature

At SG13-14 depth, creep closure rate can be expected to be $\dot{\varepsilon}_{cr} \approx$ -10^{-5}/yr (-0.001%/yr). Brine thermal-expansion coefficient is $\alpha_b = 4.4\times10^{-4}$/°C. A brine temperature decrease rate of $\dot{T}_c =$ -0.02 °C/yr would generate a relative brine volume decrease rate of $\alpha_b \dot{T}_c \approx$ -10^{-5}/yr — i.e., of the same order of magnitude as that of the cavern creep closure rate: temperature evolution must be carefully assessed to prevent severe misinterpretation. By December 2008, a temperature gauge was lowered into the SG13 well. The cavern temperature remained perfectly constant during the period December 2008 – June 2010. Gauge accuracy was tested as follows: in June 2010, cavern pressure was rapidly increased. In such a context, brine evolutions are almost perfectly adiabatic (any pressure change generates a (small) temperature change, Gatelier et al., 2008) and a ΔT (°C) $= \alpha_b T \Delta P / \rho_b C_b \approx 0.03\ \Delta P$ (MPa) temperature increase can be expected ($\rho_b C_b$ is the volumetric heat capacity of brine). In fact, gauge indication increased by 0.02°C when pressure increase reached $\Delta P_c \approx 0.6$ MPa (Figure 4) proving that the gauge was sensitive, that its resolution was 0.02°C and that temperature evolution was exceedingly slow.

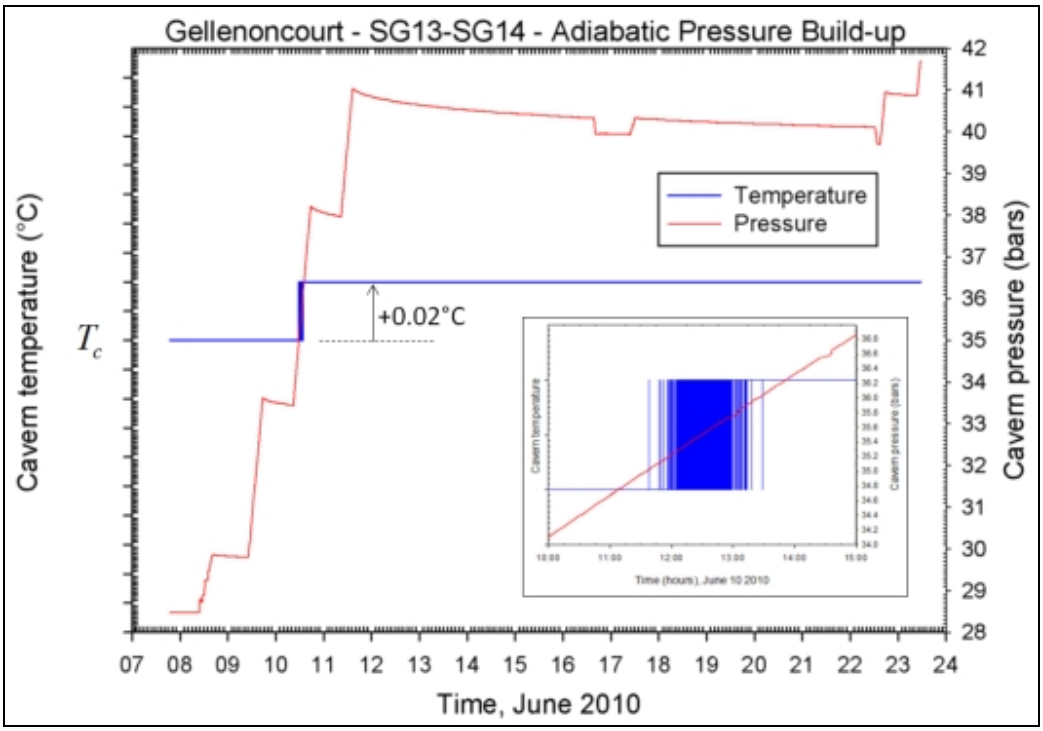

Figure 4 - Checking temperature gauge accuracy. Cavern brine warms when brine pressure increases. A pressure increase by 35 - 28.5 = 6.5 bars (900 psi) leads to an "adiabatic" temperature increase by 0.02°C (0.035°F) which is correctly observed by the temperature gauge.

3. THE BRINE OUTFLOW TEST

3.1. Average brine flow-rate

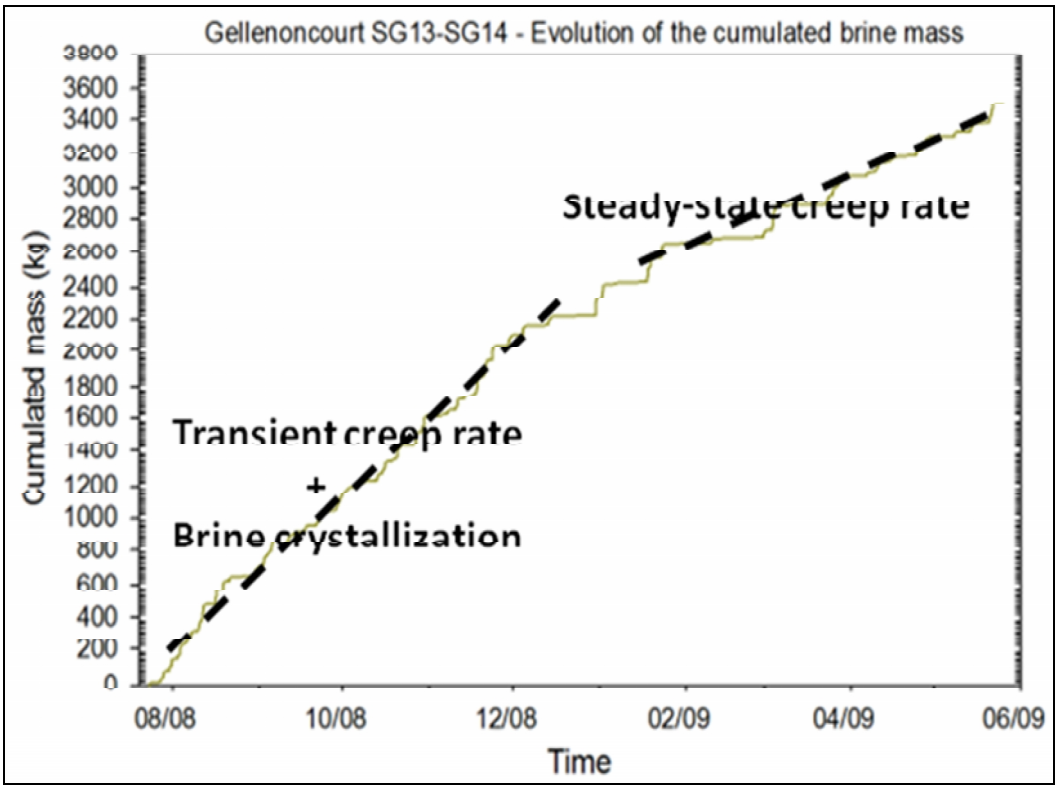

Figure 4 - Cumulated expelled mass as a function of time from July 23, 2008 to May 25, 2009.

In 2000 the cavern had been shut-in after a sonar survey. Eight years later, before the test began, wellhead pressure had built up to approximately 0.08 MPa. On July-3, 2008, the cavern was opened and wellhead pressure dropped to zero. Brine overflow was evacuated to a plastic container whose weight was measured every minute.

The outflow test began on July 23, 2008 and was completed by May 25, 2009. The *average* brine outflow rate, or $\overline{q}$, results from cavern-creep closure and cavern-brine thermal expansion:

$$\overline{q} = -\dot{\varepsilon}_{cr} V + \alpha_b \dot{T}_c V \tag{1}$$

In the case of the SG13-SG14 cavern, it was proven that temperature rate is exceedingly slow, $\left|\dot{T}_c\right| \ll \left|\dot{\varepsilon}\right| / \alpha_b$. In other words, the observed average flow-rate is representative of cavern creep closure during the test. The cumulated mass of expelled brine as a function of time is shown in Figure 5. The *average* brine-outflow rate during this 306-day long test is $\overline{q}$ = 9.5 liters/day. As cavern volume is $V = 240{,}000$ m^3, the relative creep closure rate is $\dot{\varepsilon}_{cr} = -\overline{q}/V = -4.6\times10^{-13}$ s^{-1} $= -1.45\times10^{-5}$ yr^{-1}. However brine outflow clearly decreases during the test period; a part of the initial flow was triggered by the July-3 cavern pressure drop and is transient in nature. The overall duration of the test is 306 days; during the first 200 days, transient effects, including transient creep and brine crystallization, play a significant role. During the last part of the test (from February 2009 to May 2009) cavern evolution is more representative of steady-state behavior.

3.2. Flow-rate fluctuations

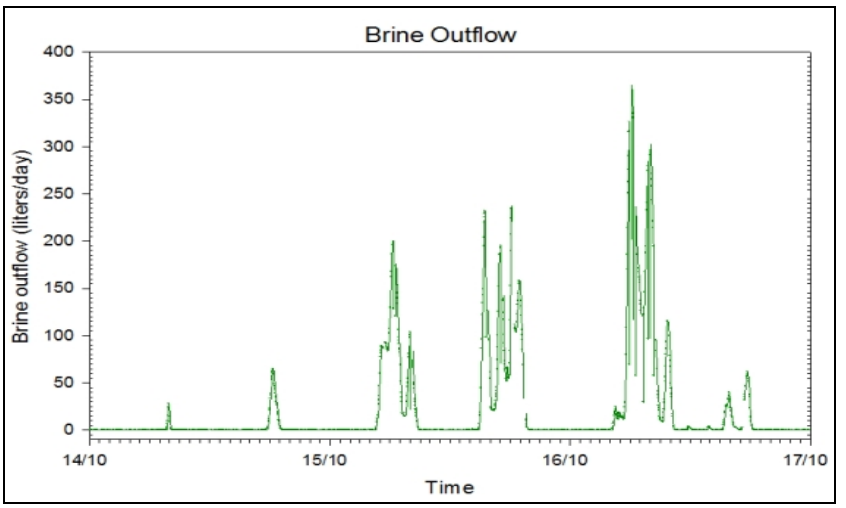

Figure 5 - Brine flow-rate from October 14 to 17, 2008.

The *average* brine flow-rate over a 10-month-long period was computed in Section 3.1. Figure 5 displays flow-rate evolution during a 3-day long period. Large fluctuations can be observed: periodically, the brine flow rate is several hundreds of liters per day. Conversely, for most of the time, the flow rate is nil and the air/brine interface drops down into the well (Figure 6). Several phenomena contribute to this apparently erratic behavior, among which atmospheric pressure variations.

3.2.1. Atmospheric pressure fluctuations

h is the height of the brine column in the well; *h* = *H* when brine is evacuated through the venting hole. Cavern pressure, or P_c, and atmospheric pressure, or P_{atm}, are related by (2), where $\rho_b g$ is brine volumetric weight:

$$P_c = \int_0^h \rho_b g dz + P_{atm} \quad \text{or} \quad \dot{P}_c = \rho_b g \dot{h} + \dot{P}_{atm} \tag{2}$$

Two cases must be considered. When brine is expelled from the cavern, $h = H$, $\dot{h} = 0$, $\dot{P}_c = \dot{P}_{atm}$ and the flow of brine is:

$$q = -\dot{\varepsilon}_{cr} V + \beta_\infty V \dot{P}_{atm} - \beta V \dot{P}_{atm} \quad ; \quad h = H \tag{3}$$

Where $-\beta_\infty V \dot{P}_{atm}$ is the cavern contraction rate generated by stress changes in the rock mass due to atmospheric pressure fluctuations and $-\beta V \dot{P}_{atm}$ is the expelled brine flow rate resulting from cavern pressure changes. Atmospheric pressure fluctuations are transmitted to the rock mass through the ground (and also through the brine column in the well). Except during a severe storm, pressure changes are almost uniform in a large horizontal domain whose dimensions are much larger than cavern depth ($H = 250$ m). Hence, at cavern depth, it can be assumed that the additional stresses generated by these fluctuations can write: $\dot{\sigma}_{zz} = -\dot{P}_{at}$ and $\dot{\sigma}_{xx} = \dot{\sigma}_{yy} = -\bar{\nu} \dot{P}_{atm} / (1 - \bar{\nu})$ where $\bar{\nu}$ is the Poisson's ratio of the rock mass. These stresses generate a cavern-volume variation of $-\beta_\infty V \dot{P}_{atm}$ where β_∞ is a function of the elastic properties of the rock mass and of the shape of the cavern.

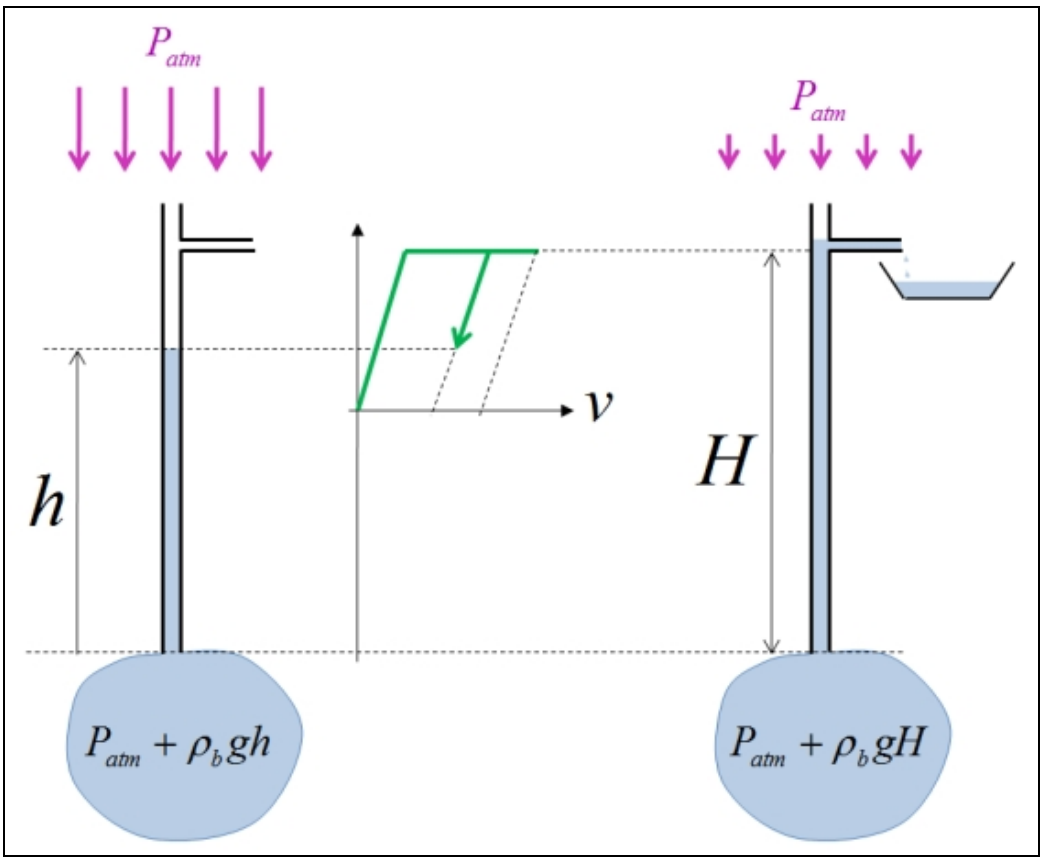

Figure 6 - Brine outflow from a shallow cavern: low atmospheric pressure and brine flow from the cavern (right); rapidly increasing atmospheric pressure with no observed brine flow (left).

Conversely, when the brine/air interface is below the venting hole, $h < H$, and:

$$S\dot{h} = -\dot{\varepsilon}_{cr} V + \beta_\infty V \dot{P}_{atm} - \beta V \dot{P}_c \; ; \qquad h < H \tag{4}$$

Combining (1) and (3) leads to:

$$\left(S + \beta V \rho_b g\right)\dot{h} = -\dot{\varepsilon}_{cr} V - \left(\beta - \beta_\infty\right) V \dot{P}_{atm} \; ; \qquad h < H \tag{5}$$

Where the cross sectional area of the well, or $S = 2.1\times10^2$ m^2, is much smaller than $\beta V \rho_b g \approx 1.56$ m^2; $\chi = \left(\beta - \beta_\infty\right)/\left(\beta + S/\rho_b g V\right) < 1$ can be compared to the "barometric efficiency", a notion defined in wells tapped in aquifer layers (Jacob 1940).

These equations prove that the cavern behaves as an extremely sensitive barometer. Equation (2) predicts that a change in atmospheric pressure by $\dot{P}_{atm}$ generates a change in brine flow rate by $q = -\left(\beta - \beta_\infty\right) V \dot{P}_{atm}$. It will be proven in that $\beta_\infty / \beta \approx 0.542$, or $q / \dot{P}_{atm} \approx$ -6 (liter/hPa). On a short time-scale, erratic fluctuations of atmospheric pressure due for instance to a sudden gust of wind (say, several dozens of Pa, or several thousandths of a psi) generate a dramatic flow-rate increase. However, atmospheric pressure fluctuations can be accurately measured and it was expected that the brine outflow rate could easily be corrected from their effects. Data processing led to relatively poor results. Several factors explain this disappointing result, as explained below.

3.2.2 Dynamic oscillations of the brine column in the well

Rapid changes in pressure trigger oscillations of the brine column in the well. Consider the case when $h = H$ (brine is expelled from the well). Equations (1) and (2) must be rewritten as follows. The mass of brine contained in the well is $\rho_b SH$. When this mass moves up and down in the well, its acceleration is $\gamma = \dot{q}/S$. When derivated with respect to time, Newton's law of motion can be written:

$$\dot{P}_c = \left[\rho_b g\dot{h} + \dot{P}_{atm}\right] + \rho_b H\ddot{q}/S \tag{6}$$

$$q = \left[-\dot{\varepsilon}_{cr}V + \beta_\infty V\dot{P}_{atm}\right] - \beta V\dot{P}_c \tag{7}$$

In the context of rapid oscillations, the terms between brackets can be disregarded. Eliminating cavern pressure between (5) and (6) leads to a second order differential equation, $(S/\beta V)q + \rho_b H\ddot{q} = 0$. This equation describes harmonic oscillations. As $\beta V\rho_b g \approx 1.56$ m^2 and $S = 2.1\times10^2$ m^2, the period of small oscillations is $\tau = 2\pi\sqrt{H\beta V\rho_b/S}$ or 4 minutes. These oscillations are slowly dampened (Bérest et al., 1999) and they blur the relation between atmospheric pressure variations and brine outflow to the container.

3.2.3. Cooling of the brine column rising inside the well

When the well is at rest, cavern brine temperature is warmer than brine geothermal temperature in the well. When brine moves upward, cool brine expelled at ground level is substituted by warm brine flowing from the cavern and the brine column in the well is made lighter, cavern pressure decreases, and brine flow is made faster. Heat exchange in the well between the rock formation and the warm brine in the well must also be taken into account. Equation (1) must be re-written in the more precise form:

$$\dot{P}_c = \int_0^H \frac{\partial\rho_b}{\partial t} g dz + \dot{P}_{atm} = \rho_b g\alpha_b \int_0^H \frac{\partial T}{\partial t}\, dz + \dot{P}_{atm} \tag{8}$$

It can be proven (see Appendix) that when warm brine starts rising in the well, brine outflow rate can be written as follows:

$$q\left(1 - \beta V\rho_b g\alpha_b \Gamma H/S\right) = -\dot{\varepsilon}_{cr}V - \left(\beta - \beta_\infty\right)V\dot{P}_{atm} \tag{9}$$

Where $\Gamma = 3\times10^{-2}$ °C/m is the geothermal gradient and $\beta V\rho_b g\alpha_b \Gamma H/S \approx 0.24$: (8) proves that brine rate is significantly accelerated when warm brine enters the well.

3.2.4 Conclusion

This analysis proves that, even if the average brine flow-rate clearly is representative of cavern behavior, flow-rate daily behavior is blurred by large fluctuations from external origin. Interpretation of the shut-in pressure test will prove to be simpler.

4 THE SHUT-IN PRESSURE TEST

4.1 Average pressure build-up rate

The cavern was shut-in from May 25, 2009 to November19, 2009. During a shut-in test, the equation which describes averaged evolutions must be re-written:

$$\overline{q} = 0 = -\dot{\varepsilon}_{cr} V - \beta V \dot{P}_c \qquad \dot{P}_c = \dot{P}_{wh} \tag{9}$$

where P_{wh} is the wellhead pressure, whose evolution is shown on Figure 7. Wellhead pressure increase during the 10-month period is 80 kPa, making the average pressure build-up rate due to cavern creep closure $\dot{P}_{wh} = -\dot{\varepsilon}_{cr}/\beta \approx 47.1$ Pa/day, from which it can be inferred that cavern closure rate is $\dot{\varepsilon}_{cr} = \dot{V}/V \approx -0.93 \times 10^{-5}$ /yr (Cavern complete closure is reached after more than 100,000 years.)

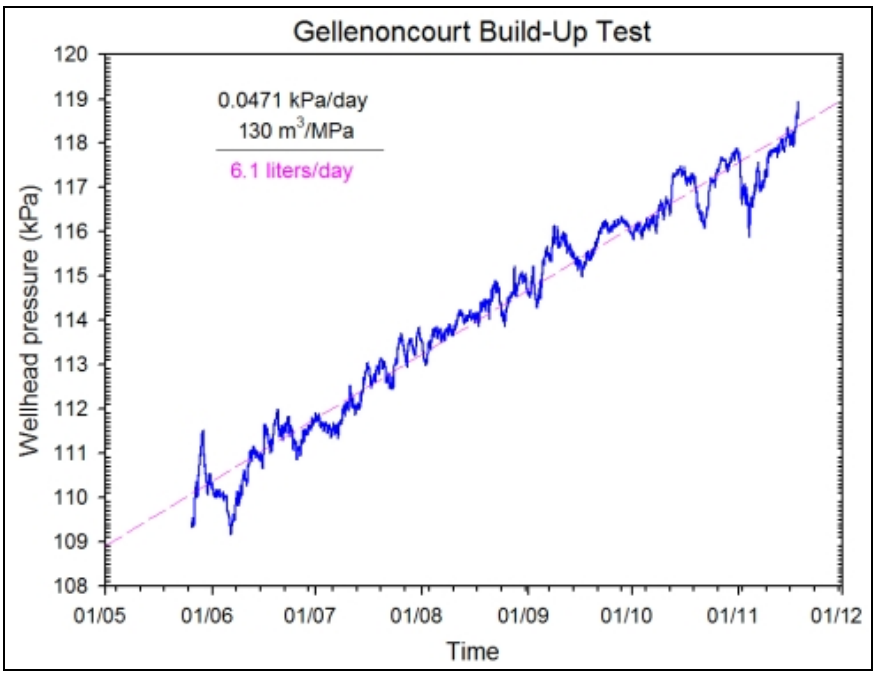

Figure 7 – Wellhead pressure evolution during the shut-in test.

4.2 Wellhead pressure fluctuations

Wellhead pressure experiences significant fluctuations. Figure 8 displays wellhead pressure and atmospheric pressure as measured during a 2-month long period. The wellhead is closed; however atmospheric pressure fluctuations are transmitted to the cavern through the rock mass, as explained above. The coefficient of empirical correlation between cavern pressure variations and atmospheric pressure variations is $\beta_\infty/\beta \approx 0.542$. Daily fluctuations in wellhead pressure generated by daily changes in ground level temperature will not be discussed here; they are relatively small. A Fourier analysis was performed and two peaks associated with Earth tides could be observed. In fact, fluctuations generated by Earth tides are visible clearly on Figure 8, for instance between September 15 and September 25, a period during which their amplitude is $\Delta P^{wh} \approx 1$ hPa, from which it can be inferred that cavern deformation is $\beta \Delta P^{wh} \approx 5 \times 10^{-8}$, a figure that is typical of the strains induced by Earth tides.

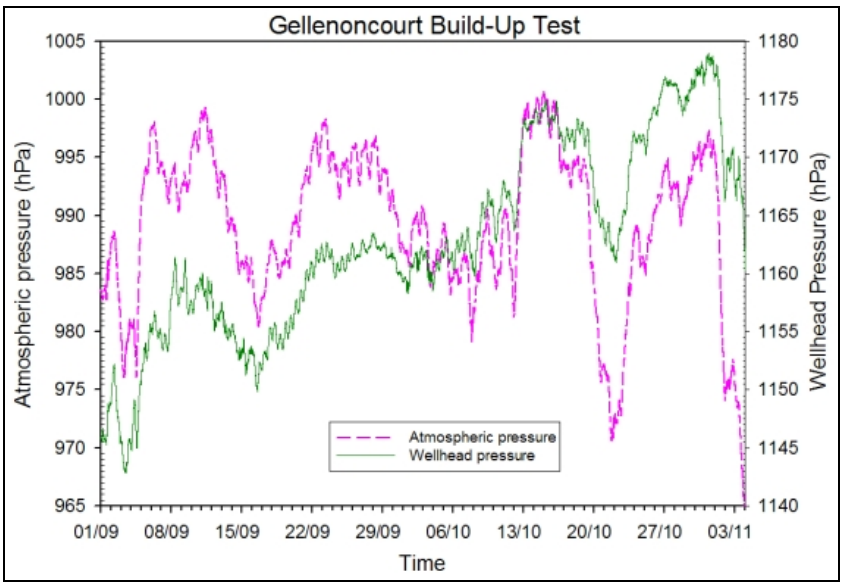

Figure 8 - Wellhead pressure and atmospheric pressure during the Sept.-Nov. 2009 period. Earth tides effects are visible clearly, for instance in the Sept. 15 to 25 period.

4.3 Steady-state cavern creep vs. transient cavern creep

It was observed during the brine outflow test that the *average* brine flow rate, computed from July 23, 2008 to May 25, 2009, was: $q/V = 1.45\times10^{-5}$ yr^{-1}. However brine flow-rate slowly decreases with time. During the shut-in test, from May 25, 2009 to November 19, 2009, the cavern creep closure rate, inferred from pressure increase rate, was slower, $-\dot{\varepsilon}_{cr} = \dot{P}/\beta = 0.93\times10^{-5}$ yr^{-1}. This last figure is more representative of steady-state creep closure rate, as transient effects are important at the beginning of the outflow test. It was mentioned that the cavern had been shut-in from 2000 to 2008; on July 2008, when the compressibility test started the wellhead pressure dropped by slightly more than $\Delta P_c = -0.08$ MPa — a small figure, but large enough to trigger various transient phenomena. Salt crystallization and transient creep are especially important. Immediately after the pressure drop, cavern brine is over-saturated in the new pressure conditions and crystallization takes place till saturation is reached again. The volume of brine expelled as a consequence of crystallization can be assessed (see Appendix B)); it is $\Delta V^{\exp} \approx 1200$ liters. Transient creep also has significant effects. It includes both the rheological transient creep, as can be observed during a standard triaxial creep test performed at the laboratory and the geometrical transient creep, or the slow redistribution of stresses in the rock mass following any cavern pressure change, an effect which is not present in the case of a uniformly loaded sample.

CONCLUSIONS

A 10-month long brine outflow test and a 6-month long shut-in test were performed in a 250-m deep salt cavern at Gellenoncourt in Lorraine, France. This cavern had been kept idle for 30 years before the tests and brine temperature changes were exceedingly small. The steady-state creep closure rate, as observed during the shut-in test, is slightly slower than 10^{-5}/year or 2 m^3/year. This value proves that even in the long term (several centuries) subsidence and possible brine leaks from the cavern should have negligible impact from the point of view of environmental protection.

REFERENCES

Bérest P., Bergues J., Brouard B. 1999. Review of static and dynamic compressibility issues relating to deep underground salt caverns. *Int. J Rock Mech Min Sci* 36:1031-1049.

Bérest P., Brouard B., Karimi-Jafari M., Van Sambeek L. 2007. Transient behavior of salt caverns – Interpretation of mechanical integrity tests. *Int J Rock Mech Min Sci*, 44:767-786.

Jacob C.E. 1940. On the flow of water in an elastic artesian aquifer. *Eos Trans AGU*, 21:574-586.

Brouard B, Bérest P, Héas JY, Fourmaintraux D, de Laguérie P, You T. 2004. An in situ test in advance of abandoning of a salt cavern. Proceedings SMRI Fall Meeting, Berlin, Germany, p 45-64.

Bérest P, Bergues J, Brouard B, Durup JG, Guerber B. 2001. A salt-cavern abandonment test. Int J Rock Mech Min Sci;38:343-55.

Buffet A. 1998. The collapse of Compagnie des Salins SG4 and SG5 drillings. Proceedings SMRI Fall Meeting, Roma, Italy, p 79-105.

Gatelier N., You T., Bérest P., Brouard B. 2008. "Adiabatic" temperature changes in an oil-filled cavern. Proceedings SMRI Fall Meeting, Austin, Texas, p 81-104.

Appendix A

Cooling of the brine column rising inside the well

When the well is at rest, cavern brine temperature, T_c, is warmer than brine temperature in the well, which is $T_0(z) = T_c - \Gamma z$; Γ is the geothermal gradient. When brine moves upward, cool brine expelled at ground level is substituted by warm brine flowing from the cavern, and the brine column in the well is made lighter, cavern pressure decreases, and brine flow becomes faster. However, heat exchange in the well between the rock formation and the warm brine in the well also must be taken into account. It is assumed that outflow takes place, $h = H$, and Equation (1) must be re-written in the more precise form:

$$P_c = \int_0^H \rho_b g dz + P_{atm} \text{ and } \dot{P}_c = \int_0^H \frac{\partial \rho_b}{\partial t} g dz + \dot{P}_{atm} = \rho_b g \alpha_b \int_0^H \frac{\partial T}{\partial t} dz + \dot{P}_{atm} \qquad \text{(A1)}$$

where $T(z,t)$ is brine temperature in the well. It is assumed that well brine was at rest when $t < 0$ (i.e., $q(t<0) = 0$) and that its temperature equaled the geothermal temperature of the rock, or $T(z, t<0) = T_0(z)$. When brine rises in the well, its temperature, $T = T(z,t)$, is slightly warmer than rock temperature, $T_R(r,z,t)$, at the same depth, and heat exchange takes place. Heat flux from the rock mass should be described by Fourier's equation for heat conduction; however, because we are interested mainly in orders of magnitude, the following simplistic model is accepted: the heat flux is assumed to be proportional to the difference between the virgin temperature of the rock and brine temperature:

$$\begin{cases} \dfrac{dT(z,t)}{dt} = \dfrac{\partial T}{\partial t}(z,t) + \dfrac{q}{S}\dfrac{\partial T}{\partial z}(z,t) = -\dfrac{1}{t_c}\left[T(z,t) - T_0(z,t)\right] \\ T(z,0) = T_0(z) = T_c - \Gamma z \qquad ; \qquad T(0,t) = T_c \end{cases} \qquad \text{(A2)}$$

where a is the well radius, $t_c \approx a^2/k_{salt}$, $k_{salt} \approx 100$ m^2/yr is the thermal diffusivity of salt, and $t_c \approx 1$ to 2 hours. This partial differential equation must be solved according to the "characteristic lines" method. When brine flow rate (q) is assumed to be approximately constant for any $t > 0$, the solution of (10) is:

$$\begin{cases} T(z,t) = T_c - \Gamma z + \Gamma q t_c \left[1 - \exp\left(-t/t_c\right)\right]/S & \text{when } z - qt/S > 0 \\ T(z,t) = T_c - \Gamma z + \Gamma q t_c \left[1 - \exp\left(-Sz/qt_c\right)\right]/S & \text{when } z - qt/S < 0 \end{cases} \quad \text{(A3)}$$

from which it can be inferred:

$$\int_0^H \frac{\partial T(z,t)}{\partial t} dz = \Gamma q \int_{qt/S}^H \exp\left(-t/t_c\right) dz/S = \left(H - qt/S\right) \Gamma q \exp\left(-t/t_c\right)/S \quad \text{when} \quad qt/S < H \quad \text{(A4)}$$

This quantity is largest at $t = 0$; at this instant, combining (A3) and (A4) leads to:

$$q\left(1 - \beta V \rho_b g \alpha_b \Gamma H/S\right) = -\dot{\varepsilon}_{cr} V - \left(\beta - \beta_\infty\right) V \dot{P}_{atm} \quad \text{(A5)}$$

$\beta V = 130$ m^3/MPa, $\Gamma = 3\times10^{-2}$ °C/m, $S = 2.1\times10^{-2}$ m^2, $H = 250$ m, and $\beta V \rho_b g \alpha_b \Gamma H/S \approx 0.24$.

Equation (A5) proves that brine rate is significantly accelerated when warm cavern brine enters the well. (Note that this model predicts that in a larger and deeper cavern ($\beta V \rho_b g \alpha_b \Gamma H/S > 1$), the cavern + well system behaves as a geyser: occasionally triggered by atmospheric pressure variations, puffs of brine are spewed from the cavern.)

Appendix B

Crystallization

Immediately after a pressure drop by $\Delta P_c = -0.08$ MPa, cavern brine is over-saturated in the new pressure conditions, and crystallization takes place. After some time, saturation is reached again, and brine density and brine concentration decrease by $\Delta\rho_b = \rho_b a_s \Delta P_c$ and $\Delta c = c\psi\Delta P_c$, respectively. (Brine concentration is the ratio between the salt mass and the salt + water mass in a given volume of brine.) Let $\Delta V_c < 0$ the volume of crystallized salt (In this context, cavern creep closure is disregarded.): $\Delta V^{\exp} > 0$ is the volume of brine expelled from the cavern because of brine crystallization; V_b is the volume of brine in the cavern + the volume of expelled brine; and $\Delta V_b = \Delta V_c + \Delta V^{\exp}$. The salt-mass and brine-mass conservation equations can be written:

$$\rho_{salt} \Delta V_c = \frac{d}{dt}\left(\rho_b V_b\right) = \rho_b V_b a_s \Delta P_c + \rho_b \Delta V_b \quad \text{(B1)}$$

$$\rho_{salt} \Delta V_c = \frac{d}{dt}\left(\rho_b c V_b\right) = \rho_b V_b c \left(a_s + \psi\right) \Delta P_c + \rho_b c \Delta V_b \quad \text{(B2)}$$

From this system, it can be inferred that

$$\Delta V^{\exp} = \frac{c}{\left(1 - c\right)} V_b \left[-\psi + \rho_b \left(a_s + \psi - c a_s\right)/\rho_{salt}\right] \quad \text{(B3)}$$

Typical values of the parameters are [14]:

$$c = 0.26,\ \rho_b = 1200 \text{ kg/m}^3,\ \rho_{salt} = 2160 \text{ kg/m}^3,\ \psi = 2.6\times10^{-4} \text{ /MPa},\ a_s = 3.16\times10^{-4} \text{ /MPa}$$

and the volume of brine expelled as a consequence of crystallization is $\Delta V^{\exp} \approx 1200$ liters. The kinetics of salt crystallization is difficult to compute; however, a significant part of it certainly took place during the July 3 to July 23 period — i.e., before the brine flow test began.